Mapping the Distribution of Outer Hair Cell Voltage-Dependent Conductances by Electrical Amputation

J. Santos-Sacchi, G.-J. Huang, and M. Wu
Sections of Otolaryngology and Neurobiology, Yale University School of Medicine, New Haven, Connecticut 06510 USA

ABSTRACT The mammalian outer hair cell (OHC) functions not only as sensory receptor, but also as mechanical effector; this unique union is believed to enhance our ability to discriminate among acoustic frequencies, especially in the kilohertz range. An electrical technique designed to isolate restricted portions of the plasma membrane was used to map the distribution of voltage-dependent conductances along the cylindrical extent of the cell. We show that three voltage-dependent currents, outward K, $I_{K,n}$, and I_{Ca} are localized to the basal, synaptic pole of the OHC. Previously we showed that the lateral membrane of the OHC harbors a dense population of voltage sensor-motor elements responsible for OHC motility. This segregation of membrane molecules may have important implications for auditory function. The distribution of OHC conductances will influence the cable properties of the cell, thereby potentially controlling the voltage magnitudes experienced by the motility voltage sensors in the lateral membrane, and thus the output of the "cochlear amplifier."

INTRODUCTION

The outer hair cell (OHC) plays a pivotal role in mammalian auditory perception (see Dallos, 1992). In addition to being one of the two sensory type cells in the organ of Corti, the OHC is capable of voltage-dependent mechanical responses that appear to provide feedback into the basilar membrane, thereby enhancing the passive mechanical vibration of the cochlear partition (Brownell et al., 1985; Ashmore, 1987; Santos-Sacchi and Dilger, 1988; Ruggero, 1992). Electrophysiological and ultrastructural evidence indicates that membrane-bound voltage sensor-motor elements control OHC length (Santos-Sacchi, 1990, 1991, 1992; Ashmore, 1990, 1992; Kalinec et al., 1992; Forge, 1991; Iwasa, 1993). These molecular motors reside predominantly within the lateral plasma membrane of the OHC (Dallos et al., 1991; Huang and Santos-Sacchi, 1993, 1994).

The voltage-dependent nature of OHC motility necessarily indicates that factors which influence the voltages generated in the cell are capable of having an impact on the cell's role in hearing. Although the driving force for OHC motility is the voltage generated by the gating of transduction channels in the stereocilia of the apical membrane (Evans and Dallos, 1993), ultimately, receptor potentials may be modulated by ionic conductances located in the basolateral membrane. A variety of ionic channel types is found in the basolateral membrane (see Ashmore, 1994), including voltage-dependent K and Ca channels (Santos-Sacchi and Dilger, 1988; Ashmore and Meech, 1986; Nakagawa et al., 1991; Housley and Ashmore, 1992). We focus here on the distribution of these voltage-dependent conductances in the cylindrical OHC, because the arrangement of such conductances within the membrane will affect the cell's cable properties and the corresponding driving force imposed on the distributed system of OHC molecular motors. We demonstrate through an electrical isolation technique that voltage-dependent ionic conductances are restricted to the basal pole of the OHC. These results augment our concept of the highly partitioned nature of the OHC membrane, i.e., that mechanoelectrical transduction (sensory) resides within the apical membrane, electromechanical transduction (motor) resides within the lateral membrane, and voltage-gated channels (and synaptic machinery) reside within the basal membrane.

Preliminary presentations of these data have been made (Santos-Sacchi, 1995; Santos-Sacchi and Huang, 1996).

METHODS

Guinea pigs were overdosed with pentobarbital. The temporal bones were removed and OHCs were isolated from the cochleas by gentle pipetting of the isolated top two turns of the organ of Corti in Ca-free medium with collagenase (0.3 mg/ml). The cell-enriched supernatant was then transferred to a 700-μl perfusion chamber, and the cells were permitted to settle onto the coverglass bottom. All experiments were performed at room temperature (~23°C). A Nikon Diaphot inverted microscope with Hoffmann optics was used to observe the cells during electrical recording. Cell lengths ranged from ~60 μm to 80 μm.

We have developed a technique for electrically amputating portions of the OHC so that characteristics of restricted areas of the plasma membrane can be analyzed in isolation (Huang and Santos-Sacchi, 1993). The technique involves a double voltage-clamp protocol with two independent clamp amplifiers. Utilizing the partitioning microchamber of Evans et al. (1991) in combination with whole-cell voltage clamp, we are able to electrically amputate that portion of the OHC housed within the chamber (see Fig. 1 *A*). That is, when identical voltage clamp stimuli are simultaneously delivered to the microchamber and the cell interior, only that portion of the membrane outside the chamber is excited. The efficiency of this amputation technique is dependent upon the seal (shunt resistance) that the microchamber makes with the OHC, and we have determined that a seal of >5–10 MΩ is sufficient and obtainable (Huang and Santos-Sacchi, 1993). By grounding the microchamber interior, the cell is put equivalently and simply under the whole-cell voltage-clamp condition. Incremental amputations were made by moving the cell into or out of the chamber with

Received for publication 24 March 1997 and in final form 28 May 1997.
Address reprint requests to Dr. Joseph Santos-Sacchi, Surgery (Otolaryngology), BML 244, Yale University School of Medicine, 333 Cedar St., New Haven, CT 06510. Tel.: 203-785-7566 (office), 203-785-5407 (lab); Fax: 203-737-2245; E-mail: joseph.santos-sacchi@yale.edu.

0006-3495/97/09/1424/06 $2.00

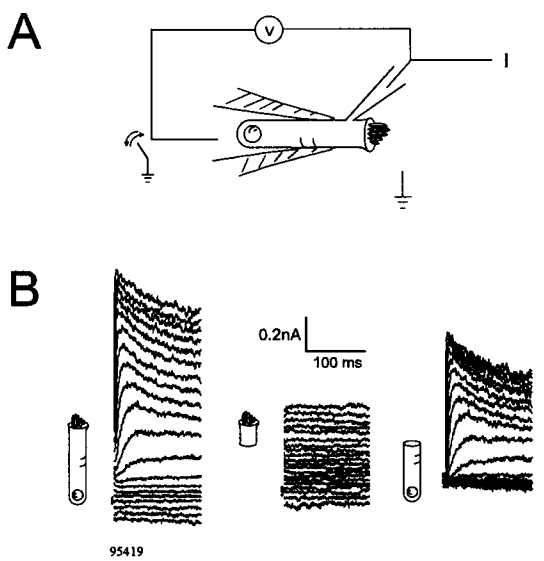

FIGURE 1 (*A*) Schematic of an outer hair cell, two-thirds of which is inserted into a microchamber and whole-cell voltage-clamped via a patch pipette. The microchamber and perfusion dish contain extracellular solution (see Methods). Identical voltage protocols are delivered to both microchamber and patch pipette to electrically isolate properties of the extruded portion of the cell. Grounding the microchamber (or clamping to zero) provides whole-cell measures. Membrane current is measured via the patch pipette. (*B*) OHC is held at −80 mV and nominally stepped from −120 to +90 mV in 10-mV increments. Series resistance corrected traces depict currents from −110 to +80 mV in 10-mV increments. Residual series resistance: 5.6 MΩ. OHC figures indicate the portion of the cell from which associated currents arise. (*Left*) Whole-cell condition. (*Middle*) Currents obtained by amputating the basal two-thirds of the cell, that is, deriving from the apical one-third of the OHC. (*Right*) Subtraction of currents resulting in those attributable to the basal two-thirds of the cell. Note that time- and voltage-dependent outward K currents are restricted to this region of the cell.

slight suction or pressure, while simultaneously moving the whole-cell patch pipette via a motorized manipulator. Fortunately, the membrane is somewhat giving, so that sometimes seals are maintained during the motion. Because the microchamber orifice diameter was smaller than initial OHC diameter and during the course of recording under whole-cell mode OHCs typically swell somewhat (cells were monitored with video), we are confident that shunt resistances remained adequate. Transmembrane currents were measured via the patch pipette. Patch pipette series resistance was estimated after the establishment of whole-cell configuration from the transient current response induced by a 10-mV step (Huang and Santos-Sacchi, 1993).

To study voltage-dependent K currents, the cells were bathed in a modified Leibovitz medium containing (in mM): NaCl 142.2, KCl 5.37, $CaCl2_2$ 2, $MgCl_2$ 1.48, HEPES 5, with 300 mOsm osmolarity (adjusted with dextrose) and pH 7.2. The intracellular solution was (in mM): KCl 140, EGTA 10, $MgCl_2$ 2, and HEPES 5, with 300 mOsm and pH 7.2. The K currents were studied at holding potentials of either −80 mV or −60 mV. The latter holding potential was used to observe $I_{K,n}$, a K current that is active at rest but deactivates at hyperpolarized potentials (Housley and Ashmore, 1992). To study the inward Ca conductance, Ba was used as the charge carrier. After the formation of whole-cell configuration in normal bath solution, barium solution (in mM: $BaCl_2$ 100, $MgCl_2$ 2, tetraethylammonium 35, 4-amino pyridine 5, CsCl 5, HEPES 10) was perfused. Intracellular solution was (in mM): CsCl 140, EGTA 10, $MgCl_2$ 2, HEPES 5. Osmolarity and pH were adjusted as above. Typically, OHCs were stepped from the holding potential in nominal increments of 10 mV to a range of potentials. For the identification of inward Ca currents, leakage subtraction was performed with the P/−4 technique.

Although averaging and subtraction of ionic currents are routinely performed to evaluate the effects of a variety of treatments, problems may arise because of residual series resistance. Essentially, current traces may not have been obtained at constant voltage. Because the OHC has a relatively low resting membrane resistance and large voltage-dependent conductances, this problem may be intensified. To overcome this problem and allow averaging and subtraction of current traces, point-by-point *I-V* curves were constructed, and each nominal voltage was corrected by subtracting the voltage drop across the series resistance. Currents at fixed voltage increments were then obtained through interpolation, so that generated current traces represented true currents at 10-mV increments. Because only interpolation was used, the complete range of corrected trace voltages was sometimes less than the nominal voltage range. Valid manipulations of current traces were then feasible. It should be noted that these corrections did not alter the experimental conclusions, because analyses without series resistance correction produced qualitatively similar results. Data collection was performed with either pClamp (Axon Instruments, CA) or a Windows-based voltage-clamp program, jClamp, both utilizing an Axon AD1200 A/D board. Analyses were performed with the software program MATLAB (Mathworks, MA) or jClamp.

RESULTS

The OHC possess a prominent voltage-dependent outward K current (Fig. 1 *B*, *left*; Ashmore and Meech, 1986; Santos-Sacchi and Dilger, 1988; Santos-Sacchi, 1989). Fig. 1 *B* (*middle*) illustrates the effects of electrically amputating the basal two-thirds of the OHC plasma membrane on the currents measured through the patch pipette; the remaining currents are attributable to the apical third of the cell. Note that activation of time- and voltage-dependent K conductances is absent. An essentially linear response is observed. The right panel demonstrates, by subtracting the apical currents from the whole-cell currents, the response of the basal two-thirds of the cell. It is clear that K currents are restricted to this area, and that little leakage current is present.

It is possible, although not at all easy, to progressively amputate smaller and smaller portions of an OHC body so that a more precise distribution of the K conductances can be obtained. Fig. 2 *A* illustrates average results ($n = 3$) from such successful single-cell amputations, where, in each case, four successive amputations were accomplished. The left panel depicts the whole-cell current before each partitioning condition. Slight changes in what appears to be leakage conductance are probably produced by the inescapable trauma of cell manipulation. Nevertheless, these relatively small effects are essentially eliminated by the resultant current subtractions that follow. The middle panel shows the currents generated by the apical portions of the cells as the amputation is restricted to more basal regions. Note that voltage-dependent conductances are progressively uncovered as the amputation is lessened. The right panel reveals, through subtraction as in Fig. 1, the decrease in K current magnitude as measures are restricted to smaller and smaller regions of the basal pole. In Fig. 2 *B*, the *I-V* plot obtained from the right panel emphasizes that reductions in K current are not observed until amputation falls below the supranuclear region; this, of course, indicates that the voltage-dependent K conductance of the OHC resides below the

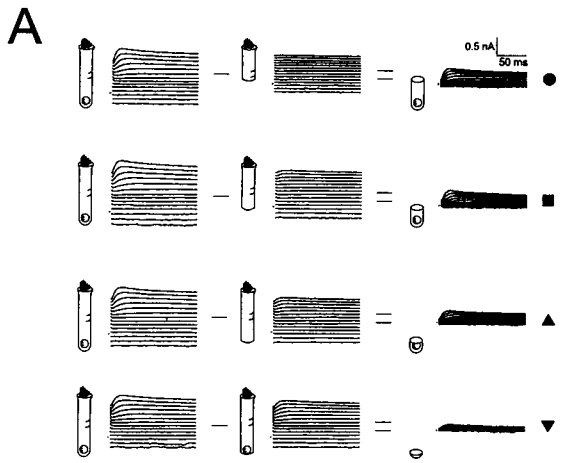

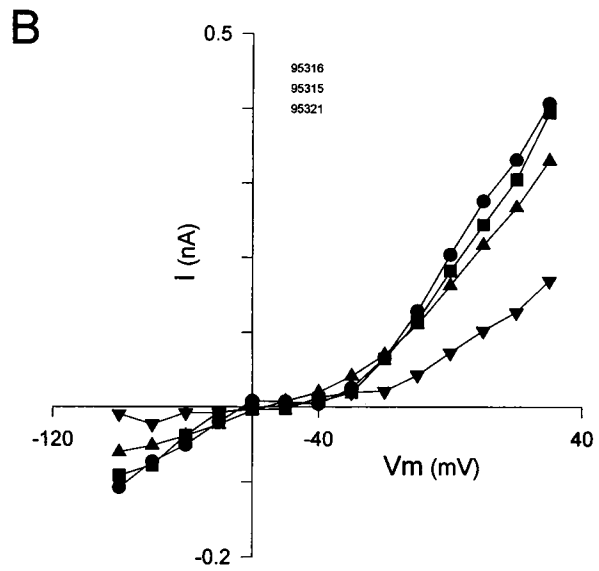

FIGURE 2 (*A*) Series resistance corrected and averaged current traces from three cells, each of which was successfully amputated at four positions. Each OHC was held at −80 mV and nominally stepped from −120 to +90 mV in 10-mV increments. Corrected traces depict currents from −100 to +30 mV in 10-mV increments. Average residual series resistance: 8.38 MΩ. OHC figures indicate portion of cell from which associated currents arise. (*Left*) Whole-cell condition obtained before amputation. (*Middle*) Apically restricted currents obtained by amputating four incrementally larger portions of the OHC's base. (*Right*) Subtraction of currents resulting in those attributable to the basal portions of the cell. (*B*) Peak current versus step potential obtained from the traces in *A*, right panel.

supranuclear region. Fig. 3 summarizes the results of electrical amputation by further subtracting the current traces to provide discrete localization of K currents along the basal extent of the cell. A total of 13 additional cells, where at least two incremental amputations were made, provided similar results.

Another prominent OHC K current that is active near rest and is believed to govern the cell's resting potential (Housley and Ashmore, 1992) is that of $I_{K,n}$. The current is characterized by a nearly instantaneous onset upon step

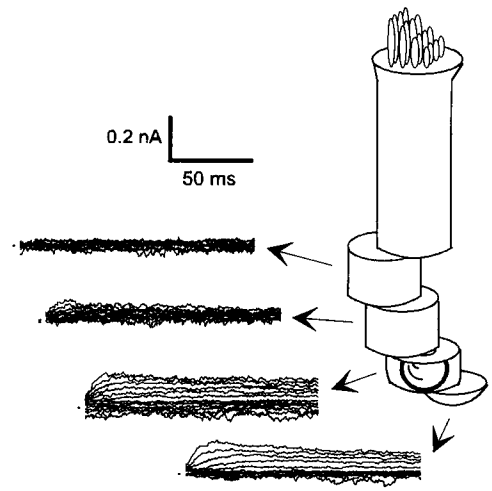

FIGURE 3 Localization of outward K currents along the basal extent of the OHC. Currents from the illustrated sections of the OHC were obtained by subtraction of currents in Fig. 2 *A*, right panel. From apical to basal, the currents correspond to (symbols in Fig. 2 *A*): circle-square, square-upward triangle, upward triangle-downward triangle, and simply downward triangle. The bulk of K conductances are restricted to the basal, nuclear region of the OHC.

hyperpolarizations from somewhat positive holding potentials (> −60 mV). The current deactivates upon hyperpolarization with a fairly long time constant that is variable among cells. Thus, while $I_{K,n}$ contributed to those currents studied above at the holding potential of −80 mV it was considerably deactivated. Fig. 4 exemplifies the effect of electrical amputation on OHCs whose $I_{K,n}$ is robust, because for these experiments holding potential was −60 mV. In this case, amputation was made slightly above the nucleus, and it is clear that the principal location of $I_{K,n}$ is within the basally amputated region, corresponding to the location of outward K currents. Six additional cells, with varying extents of $I_{K,n}$, were successfully amputated at the same level and provided similar results.

The OHC possesses a small, noninactivating Ca conductance that is revealed by leakage subtraction (Fig. 5) (Santos-Sacchi and Dilger, 1988; Nakagawa et al., 1991). Fig. 5 presents the averaged results (n = 4) of amputation experiments designed to localize Ca conductances. In these experiments, amputation of the basal pole of the cell successfully and reversibly removed the inward Ba currents, indicating that the Ca conductance colocalizes with K conductances.

DISCUSSION

Hair cells, like other nonsensory epithelial cells, are polarized morphologically and functionally. The apical and basolateral membranes of hair cells are specialized for mechanoreception and synaptic transmission, respectively (Hudspeth, 1989). Stereocilia, which are modified microvilli, are confined to the hair cell's apical region, where they serve to gate mechanically sensitive ion channels.

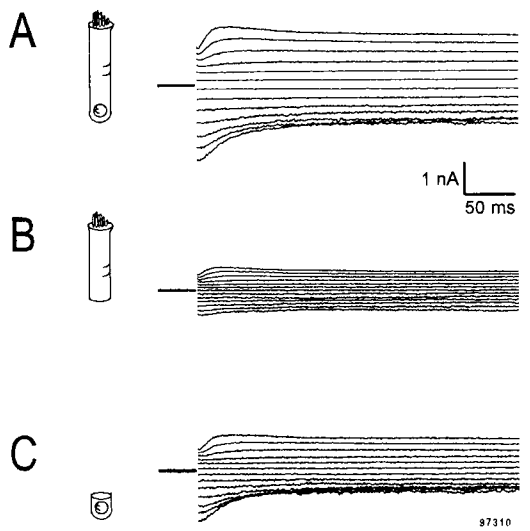

FIGURE 4 OHC held at −60 mV and nominally stepped from −140 to +10 mV in 10-mV increments. Series resistance-corrected traces depict currents from −125 to +5 mV in 10-mV increments. Residual series resistance: 6.5 MΩ. OHC figures indicate portion of cell from which associated currents arise. (*A*) $I_{K,n}$ is observed upon hyperpolarization with an instantaneous onset and slow deactivation. Outward K currents are also observed upon depolarization. (*B*) Amputation of the basal, nuclear pole of the OHC results in a nearly complete removal of $I_{K,n}$ and outward K currents. (*C*) Subtraction of apical currents (*B*) from whole cell currents (*A*) reveals those currents attributable to the basal, nuclear pole of the OHC. It is clear that $I_{K,n}$ resides in the same location as the outward K currents.

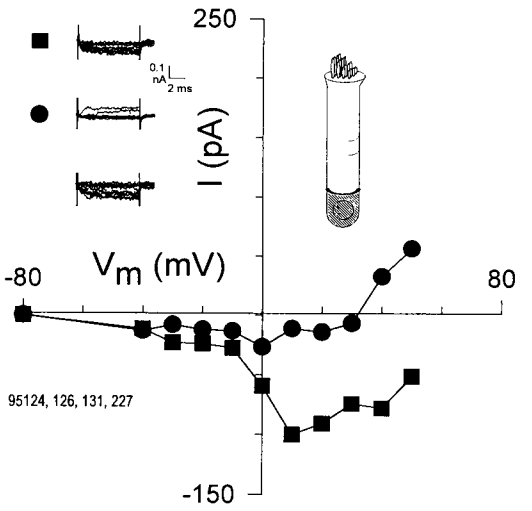

FIGURE 5 Localization of voltage-dependent Ca conductance. Average results from four cells. OHCs were held at −80 mV and stepped nominally from −40 to +40 mV in 10-mV increments. Leakage subtraction was performed with the P/−4 protocol to reveal inward Ba currents. Because the currents were so small, no correction for residual series resistance was made. Average residual series resistance: 8.25 MΩ. The *I-V* plot was obtained from the top two averaged sets of traces in the upper left; data points were averages of the final 4 ms of the current traces. Squares indicate currents obtained before amputation, and circles indicate currents obtained after amputation of the basal, nuclear pole, as indicated in the figure of the OHC. The bottom set of traces was obtained after return to whole-cell conditions. These data indicate that the OHC Ca conductance resides in the same region as the voltage-dependent K conductances.

Gating of these channels generates receptor potentials and ultimately leads to calcium-dependent neurotransmitter release onto eighth nerve afferents. Furthermore, the outer hair cell's lateral membrane serves an electromechanical function. OHCs generate voltage-dependent mechanical responses, the frequency limit (> 20 kHz) of which is currently imposed by measurement techniques (Santos-Sacchi, 1992; Dallos and Evans, 1995). Membrane-bound sensormotor elements responsible for this unique motility have been localized to the central extent of the OHC's cylindrical soma, namely between apical cuticular plate and basal, nuclear region (Dallos et al., 1991; Huang and Santos-Sacchi, 1993). Gating current studies indicate that the density of molecular motors within the OHC lateral membrane is ~7500/μm^2 (Huang and Santos-Sacchi, 1993); this is in line with morphological evidence showing similar densities of 10-nm intramembranous particles, the putative molecular motors (Forge, 1991). It is clear that the lateral membrane of the OHC, unlike that of other types of hair cells, is uniquely specialized.

It is demonstrated here that the voltage-dependent K and Ca conductances of the OHC are not distributed within the plasmalemma along the entire length of the cell, but instead are restricted to the basal, synaptic pole. The cellular mechanisms that direct and maintain the segregation of molecular motors to the lateral membrane and ionic channels to the basal membrane possibly involve the extensive cortical cytoskeleton found in OHCs (Holley and Ashmore, 1988). Disruption of the cytoskeleton might promote intermixing of the molecules, which could be identified electrophysiologically. It is important to note that the K conductances were not amputated, because of a simultaneous removal of a required Ca influx. Although a component of the outward K current may be Ca-dependent, the bulk of this current is not (Santos-Sacchi, 1989). Recently this independence from Ca was confirmed and, in addition, it was shown that $I_{K,n}$ is little affected by the removal of extracellular calcium (Mammano and Ashmore, 1996; Nenov et al., 1997). Thus, electrical amputation of the K as well as Ca currents in this study is due almost exclusively to direct removal of the voltage stimulus to the channels' voltage sensors.

After the identification of a noninactivating L-type Ca current in OHCs (Santos-Sacchi and Dilger, 1988; Santos-Sacchi, 1989), other detailed examinations, including a localization study, of the conductance were made (Nakagawa et al., 1991, 1992). Focal Ca channel blocker application demonstrated that Ca current blockade occurred primarily during application to the basal pole of the OHC. This is in line with the results of the present experiments. Similar $I_{K,n}$ localization studies by these investigators, using focal application of the blocker Ba, indicated that $I_{K,n}$ is distributed along the length of the OHC (Nakagawa et al., 1994). Our data, however, present a more restricted localization of $I_{K,n}$ at the basal pole of the OHC. Focal application ("puffer") studies may sometimes suffer from diffusion of drugs away

from sites of presumed application. Earlier studies in lower-vertebrate hair cells, using unequivocal localization methods, demonstrated that Ca-activated K and Ca conductances are colocalized to synaptic sites along the full extent of the basolateral membrane of these cells (Issa and Hudspeth, 1994; Roberts et al., 1990). In addition to a role in synaptic function, the clustering of these conductances may be required for the electrical tuning found in these nonmammalian hair cells. Electrical resonance is not found in mammalian auditory hair cells, and in the case of the OHC it has been suggested that the Ca-independence of the outward K current might preclude such oscillatory behavior (Santos-Sacchi, 1989). Also unlike lower vertebrate hair cells, OHC synaptic sites are restricted to the basal, nuclear region of the plasma membrane—the same region where voltage-dependent K and Ca conductances reside. Thus it is conceivable that the K and Ca conductances of the OHC, as in lower-vertebrate hair cells, are associated with afferent and/or efferent synaptic sites. Whereas it is clear that efferent synaptic functionality is robust based on a host of indirect physiological studies (e.g., Brown et al., 1983), the functionality of the meager afferent supply to the OHC, which most likely has never been recorded from, remains questionable (Liberman, 1982; Robertson, 1985). The contribution of K and Ca conductances to synaptic activity of the OHC must await direct studies of this issue.

Many characteristics of OHCs are correlated with cell length. Although we did not study the effects of cell length on conductance distribution, it is likely that the basic compartmentalization of the OHC remains the same, regardless of length. Indeed, regardless of length, it is clear, for example, that mechanically gated transduction channels are restricted to the cell apex, synapses are restricted to the basal pole, and subsurface cisternae line the lateral membrane. One of the characteristics that does depend on cell length is the occurrence of $I_{K,n}$ (Housely and Ashmore, 1992), with the whole-cell conductance being greater in shorter cells. All of our cells were between ~60 μm and 80 μm, but the occurrence of $I_{K,n}$ in cells of this length range is not clearly dependent on cell length. In 83 cells studied, 43 were found to have observable $I_{K,n}$ (length: 68.26 $\pm$ 1.2 μm [mean $\pm$ SE]; zero current potential [after pipette-cell solution equilibration]: -57.5 ± 1.4 mV). The remaining cells lacked observable $I_{K,n}$ (length: 64.1 $\pm$ 0.8 μm; zero current potential: -39.8 ± 1.5 mV). Thus, in this length range there appears to be little dependence of $I_{K,n}$ on cell length. Note, however, that this is not in disagreement with the data of Housley and Ashmore (1992), where clear dependence of OHC conductance on length is not obvious in this restricted range of length.

Given the conductance localization pattern in the OHC, it is possible to draw some conclusions about ionic channel density. The length, unlike the constant width (10 μm), of OHCs is inversely related to its characteristic frequency, ranging in the guinea pig from ~80 μm (~200 Hz) to 20 μm (~40,000 Hz). Whereas the surface area of the lateral membrane is directly related to the cell's length, the surface area of the basal, synaptic pole remains roughly constant. As noted above, the K current density of OHCs has been shown to increase as cell length decreases (Housley and Ashmore, 1992). Clearly, then, K channel density must increase, not as a consequence of reduced surface area, but as a consequence of an increased channel population. Interestingly, we have recently shown that motility gating current density and intramembranous particle density in the lateral membrane increase as length decreases (Kakehata et al., 1997). The higher density of these molecules (channels and molecular motors) in high-frequency OHCs probably corresponds to the enhanced frequency tuning afforded by these cells in the high-frequency region of the cochlea.

Finally, the voltage-dependent ionic channel distribution determined here necessarily limits the conductances' influence on local voltage drops across the lateral membrane, where the motility voltage sensors reside. The OHC lateral wall (subsurface cisternae, cortical cytoskeleton, and plasma membrane) is a complex structure with electrical properties that are equally complex (Pollice and Brownell, 1993; Kruger et al., 1997). Nevertheless, the absence of current shunting in the lateral membrane may ensure that voltages generated there (viz., the driving force for the "cochlea amplifier") will be largely unaffected by remote conductance changes in the basal pole of the cell.

We thank Margaret Mazzucco for technical help.

This work was supported by National Institutes of Health-NIDCD grant DC00273 to JSS.

REFERENCES

Ashmore, J. F. 1987. A fast motile response in guinea-pig outer hair cells: the cellular basis of the cochlear amplifier. *J. Physiol. (Lond.).* 388: 323–347.

Ashmore, J. F. 1990. Forward and reverse transduction in the mammalian cochlea. *Neurosci. Res. Suppl.* 12:S39–S50.

Ashmore, J. F. 1992. Mammalian hearing and the cellular mechanism of the cochlear amplifier. *In* Sensory Transduction. D. P. Corey and S. D. Roper, editors. Rockefeller University Press, New York. 395–412.

Ashmore, J. F. 1994. The G. L. Brown Prize Lecture. The cellular machinery of the cochlea. *Exp. Physiol.* 79:113–134.

Ashmore, J. F., and R. W. Meech. 1986. Ionic basis of membrane potential in outer hair cells of guinea pig cochlea. *Nature.* 322:368–371.

Brown, M. C., A. L. Nuttall, and R. I. Masta. 1983. Intracellular recordings from cochlear inner hair cells: effects of stimulation of the crossed olivocochlear efferents. *Science.* 222:69–72.

Brownell, W. E., C. R. Bader, D. Bertrand, and Y. de Ribaupierre. 1985. Evoked mechanical responses of isolated cochlear outer hair cells. *Science.* 227:194–196.

Dallos, P. 1992. The active cochlea. *J. Neurosci.* 12:4575–4585.

Dallos, P., and B. N. Evans. 1995. High-frequency motility of outer hair cells and the cochlear amplifier. *Science.* 267:2006–2009.

Dallos, P., B. N. Evans, and R. Hallworth. 1991. On the nature of the motor element in cochlear outer hair cells. *Nature.* 350:155–157.

Evans, B. N., and P. Dallos. 1993. Stereocilia displacement induced somatic motility of cochlear outer hair cells. *Proc. Natl. Acad. Sci. USA.* 90:8347–8351.

Evans, B. N., R. Hallworth, and P. Dallos. 1991. Outer hair cell electromotility: the sensitivity and vulnerability of the DC component. *Hear. Res.* 52:288–304.

Forge, A. 1991. Structural features of the lateral walls in mammalian cochlear outer hair cells. *Cell Tissue Res.* 265:473–483.

Holley, M. C., and J. F. Ashmore. 1988. Spectrin, actin and the structure of the cortical lattice in mammalian cochlear outer hair cells. *J. Cell Sci.* 96:283–291.

Housley, G. D., and J. F. Ashmore. 1992. Ionic currents of outer hair cells isolated from the guinea-pig cochlea. *J. Physiol. (Lond.).* 448:73–98.

Hudspeth, A. J., 1989. How the ear's works work. *Nature.* 341:397–404.

Huang, G.-J., and J. Santos-Sacchi. 1993. Mapping the distribution of the outer hair cell motility voltage sensor by electrical amputation. *Biophys. J.* 65:2228–2236.

Huang, G.-J., and J. Santos-Sacchi. 1994. Motility voltage sensor of the outer hair cell resides within the lateral plasma membrane. *Proc. Natl. Acad. Sci. USA.* 91:12268–12272

Issa, N. P., and A. J. Hudspeth. 1994. Clustering of Ca^{2+} channels and Ca^{2+}-activated K^+ channels at fluorescently labeled presynaptic active zones of hair cells. *Proc. Natl. Acad. Sci.* USA. 91:7578–7582.

Iwasa, K. H. 1993. Effect of stress on the membrane capacitance of the auditory outer hair cell. *Biophys. J.* 65:492–498.

Kakehata, S., J. Santos-Sacchi, T. Kikuchi, and Y. Katori. 1997. Higher frequency outer hair cells have a greater specific voltage-dependent capacitance. Midwinter Meeting of the Association for Research in Otolaryngology, St. Petersburg, FL, February 1997.

Kalinec, F., M. C. Holley, K. H. Iwasa, D. J. Lim, and B. Kachar. 1992. A membrane based force generation mechanism in auditory sensory cells. *Proc. Natl. Acad. Sci. USA.* 89:8671–8675.

Kruger, R. P., M. J. Yium, J. A. Halter, and W. E. Brownell. 1997. Outer hair cell electrophysiology: modeling the electrical properties of the subsurface cisterna. Midwinter Meeting of the Association for Research in Otolaryngology, St. Petersburg, FL, February 1997.

Liberman, M. C. 1982. Single neuron labeling in the cat auditory nerve. *Science.* 216:1239–1241.

Mammano, F., and J. F. Ashmore. 1996. Differential expression of outer hair cell potassium currents in the isolated cochlea of the guinea pig. *J. Physiol. (Lond.).* 496.3:639–646.

Nakagawa, T., S. Kakehata, N. Akaike, S. Komune, T. Takasaka, and T. Uemura. 1991. Calcium channel in isolated outer hair cells of guinea pig cochlea. *Neurosci. Lett.* 125:81–84.

Nakagawa, T., S. Kakehata, N. Akaike, S. Komune, T. Takasaka, and T. Uemura. 1992. Effects of Ca^{2+} antagonists and aminoglycoside antibiotics on Ca^{2+} current in isolated outer hair cells of guinea pig cochlea. *Brain Res.* 580:345–347.

Nakagawa, T., S. Kakehata, T. Yamamoto, N. Akaike, S. Komune, and T. Uemura. 1994. Ionic properties of $I_{K,n}$ in outer hair cells of guinea pig cochlea. *Brain Res.* 661:293–297.

Nenov, A. P., C. Norris, and R. P. Bobbin. 1997. Outwardly rectifying currents in guinea pig outer hair cells. *Hear. Res.* 105:146–158.

Pollice, P. A., and W. E. Brownell. 1993. Characterization of the outer hair cell's lateral wall membranes. *Hear. Res.* 70:187–196.

Roberts, W. M., R. A. Jacobs, and A. J. Hudspeth. 1990. Colocalization of ion channels involved in frequency selectivity and synaptic transmission at presynaptic active zones of hair cells. *J. Neurosci.* 10:3664–3684.

Robertson, D. 1985. Brainstem location of efferent neurons projecting to the guinea pig cochlea. *Hear. Res.* 20:79–84.

Ruggero, M. A. 1992. Responses to sound of the basilar membrane of the mammalian cochlea. *Neurobiology.* 2:449–456.

Santos-Sacchi, J. 1989. Calcium currents, potassium currents, and the resting potential in isolated outer hair cells. Midwinter Meeting of the Association for Research in Otolaryngology, St. Petersburg, FL, February 1989.

Santos-Sacchi, J. 1990. Fast outer hair cell motility: how fast is fast? *In* The Mechanics and Biophysics of Hearing. P. Dallos, C. D. Geisler, J. W. Matthews, M. A. Ruggero, and C. R. Steele, editors. Springer-Verlag, Berlin. 69–75.

Santos-Sacchi, J. 1991. Reversible inhibition of voltage dependent outer hair cell motility and capacitance. *J. Neurosci.* 11:3096–3110.

Santos-Sacchi, J. 1992. On the frequency limit and phase of outer hair cell motility: effects of the membrane filter. *J. Neurosci.* 12:1906–1916.

Santos-Sacchi, J. 1995. Electrical dissection of ionic conductances in the outer hair cell. Symposium on the Molecular Biology of Hearing and Deafness, Bethesda, MD, October 6–8, 1995. 125.

Santos-Sacchi, J., and J. P. Dilger. 1988. Whole cell currents and mechanical responses of isolated outer hair cells. *Hear. Res.* 35:143–150.

Santos-Sacchi, J., and G.-J. Huang. 1996. Electrical dissection of ionic conductances in the outer hair cell. Midwinter Meeting of the Association for Research in Otolaryngology, St. Petersburg, FL, February 1996.